Atmospheric Environment Vol. 20, No. 6, pp. 1121–1130, 1986.
Printed in Great Britain.

0004–6981/86 $3.00
Pergamon Journals Ltd.

J-15
17

A NEW MIXED SEGMENT-PUFF APPROACH FOR DISPERSION MODELING

PAOLO ZANNETTI*
AeroVironment Inc., 825 Myrtle Avenue, Monrovia, CA 91016, U.S.A.

(*First received* 22 *July* 1985 *and received for publication* 19 *November* 1985)

Abstract—This paper presents a new mixed methodology for realistic and cost-effective simulation of short-term air quality dispersion phenomena using the Gaussian formula. The method can be applied to short-range, intermediate and, especially, long-range transport simulations. Pollutant dynamics are described by the temporal evolution of plume elements, treated as segments or puffs according to their size. While the segments provide a numerically fast simulation during transport conditions, the puffs allow a proper simulation of calm or low-wind situations.

The methodology is incorporated into a computer package (AVACTA II, Release 3) that gives the user large flexibility in defining the computational domain, the three-dimensional meteorological and emission input, the receptor locations, and in selecting plume rise and sigma formulas. AVACTA II provides both pollutant concentration fields and dry/wet deposition patterns. The model uses linear chemistry and is applicable to any two-species reaction chain (e.g., SO_2 and SO_4^{2-}) where this approximation is reasonable and an appropriate reaction rate is available.

Key word index: Air pollution, Gaussian model, puff model, long-range transport, Lagrangian modeling.

1. INTRODUCTION AND OVERVIEW

The development of air quality modeling techniques in the last 20 years has been quite remarkable. With the parallel growth in computational capabilities, it has been possible to define and implement extremely advanced simulation techniques. Nevertheless, in spite of the above improvements and expansions, it has been found that often the more complex methodologies possess only a theoretical (or potential) capability of better representing the complexities of the real world. In fact, recent important model validation studies, such as the Electric Power Research Institute (EPRI) Plume Model Validation and Development (PMV&D) Study (for example, see Liu and Moore, 1984), show that when models are applied in an operational, 'hands off' manner:

1. short-term modeling simulations are substantially inaccurate with errors of a factor of two in more than 50% of the cases;
2. the more complex modeling approaches do not provide a substantial improvement in reproducing reality, compared with the more simple ones.

This behaviour has been recently confirmed by several studies presented at the Department of Energy/American Meteorological Society Model Evaluation Workshop (Kiawah Island, SC, October 1984) in which model outputs have been evaluated against three reliable tracer experiment data bases: MATS (Mesoscale Atmospheric Transport Studies, by the Savannah River Laboratory), PMV&D (Plume Model Validation and Development study, by the Electric Power Research Institute), and ASCOT (Atmospheric Studies in Complex Terrain, by the U.S. Department of Energy).

These results indicate the need of additional air pollution modeling effort for improving the present simulation capabilities and allowing the models to reach that level of performance that is expected from them, especially for regulatory applications since air pollution dispersion models are the only tool for inferring a quantitative deterministic relation between anthropogenic pollutant emissions and ambient concentrations. Future model development efforts should aim at (1) the development and application of more complex and sophisticated methodologies, generally requiring more advanced meteorological information; e.g., particle methods (Zannetti, 1984) or higher order closure techniques (Lewellen and Teske, 1976); and (2) the improvement of the simulation capabilities of relatively simple current techniques, mainly using the available meteorological information.

The modeling discussion presented in this paper aims at the second objective above, and presents a new methodology which is able to simulate complex dispersion conditions in both transport and calm situations while maintaining the simplicity of the basic Gaussian equation. This method is computationally cost effective and allows a non-stationary, non-homogeneous representation of atmospheric phenomena such as transport, turbulent diffusion, dry and wet deposition, and first-order reaction chemistry. This mixed segment/puff approach provides an improved simulation

*Most of this research was performed by the author in the course of consulting activity in 1984 at the Center for Thermal and Nuclear Research (CRTN) of the National Electric Power Industry (ENEL) in Milan, Italy.

tool for practical applications in both short-range and long-range air pollution dispersion studies, in either flat or complex terrain. This methodology seems particularly useful for simulating long-range transport of sulfur species (SO_2, SO_4^{2-}). Model validation studies are under development and their results will be presented in successive papers.

The most widely applied air pollution models are based on the Gaussian plume equation (for example, Turner, 1970) which, in its simplest form, describes the average steady-state concentration $\chi(\mu g\, m^{-3})$ produced at the receptor $\mathbf{r} = (x_r, y_r, z_r)$ by a single point source at $\mathbf{s} = (0, 0, z_s)$ as

$$\chi = \frac{10^9 Q}{2\pi u \sigma_h \sigma_z} \exp\left[-\frac{y_r^2}{2\sigma_h^2}\right] \exp\left[-\frac{(z_s + \Delta h - z_r)^2}{2\sigma_z^2}\right] \quad (1)$$

where Q is the pollutant emission rate ($kg\, s^{-1}$), Δh is the plume rise (m), u is the average wind speed at z_s ($m\, s^{-1}$), and σ_h^* and σ_z (m) are the horizontal and vertical plume standard deviations at the downwind distance $d = x_r$ (m). The plume rise Δh and the standard deviations σ_h and σ_z can be evaluated from several semi-empirical formulae requiring meteorological and emission information. The positive x-axis is chosen to coincide with the average wind direction at z_s. The concentration χ is assumed equal to zero (or to a background value) for negative values of x_r.

Equation (1) is often expanded with (1) partial or total reflection terms at the ground and at the top of the mixing layer; (2) exponential reduction terms, for simulating dry/wet deposition and first-order chemical transformation; and (3) particle settling velocity. Moreover, it can be spatially integrated for simulating segment, area, and volume sources. Finally, Equation (1) can be rewritten in a climatological form (for example, Martin, 1971) for simulating long-term concentration averages using the combined frequency distribution of the major meteorological variables, such as wind speed, wind direction and atmospheric stability.

This steady-state formulation, however, is valid only during transport conditions (for example, $u \geq 1\, m\, s^{-1}$) in fairly stationary and homogeneous situations. In order to remove these limitations, while still maintaining the simplicity of the Gaussian approach, two dynamic methods have been developed:

1. the segmented plume model (for example, Hales *et al.*, 1977; Benkley and Bass, 1980; Chen *et al.*, 1979), which, however, still requires transport conditions;
2. the puff model (for example, Lamb, 1969; Roberts *et al.*, 1970), which can theoretically work in calm or low-wind conditions.

Both methods break the plume into independent elements (segments or puffs) whose initial features and dynamics are a function of local time-varying emissions and meteorological conditions. Therefore, they are able to simulate non-stationary and non-homogeneous dispersion conditions.

Segments are sections of a Gaussian plume. Each segment generates a concentration field which is still basically computed by Equation (1), and represents the contribution of the entire virtual plume passing through that segment, as illustrated in Fig. 1. Therefore, only one segment (the closest) affects the concentration computation at each receptor, although the occurrence of 180° wind direction changes can create particular conditions where the contribution of two segments (that is, two virtual plumes) should be superimposed at some receptors.

Puff models, on the other hand, generate a concentration field $\chi(\mu g\, m^{-3})$, which is always produced by superimposing the contribution of each single puff, given by the basic formula

$$\chi = \frac{10^9 M}{(2\pi)^{3/2}\sigma_h^2 \sigma_z} \exp\left[-\frac{(x_p - x_r)^2}{2\sigma_h^2}\right] \times \exp\left[-\frac{(y_p - y_r)^2}{2\sigma_h^2}\right] \exp\left[-\frac{(z_p - z_r)^2}{2\sigma_z^2}\right] \quad (2)$$

in which M is the mass (kg) of pollutant of the puff whose center is located at $\mathbf{p} = (x_p, y_p, z_p)$ and whose standard deviations (m) are σ_h in the horizontal and σ_z in the vertical. As with Equation (1), Equation (2) is often expanded with reflection and deposition terms. Note that Equation (2) differs from Equation (1) mainly because the transport term is replaced by an extra horizontal diffusion term with the consequent disappearance of the wind speed u. In a puff model, the wind speed affects the concentration computation only by controlling the density of puffs in the region (that is, the lower the wind speed, the closer a puff is to the next one generated by the same source), and not directly through Equation (2). Therefore, at least in theory, a puff model can handle calm or low-wind conditions. This approach represents an advanced and powerful application of the Gaussian formula.

Several studies have discussed in detail the puff modeling approach, improving its application features. In particular, (1) algorithms were proposed and evaluated for incorporating wind shear effects (Sheih, 1978); (2) virtual distance (Ludwig *et al.*, 1977) and virtual age (Zannetti, 1981) computations were defined for correctly evaluating the σ_h and σ_z dynamics of the puff; (3) puff merging (Ludwig *et al.*, 1977) or puff splitting (Zannetti, 1981) were incorporated for performing cost-effective simulations with relatively large Δt (for example, 5–10 min); and (4) an empirical method was derived (Zannetti, 1981) for evaluating the puff's σ_h and σ_z growth during calm or low-wind conditions as a function of currently available σ functions during transport conditions (this method is presented and expanded in Appendix A).

Numerically correct applications of the puff model are computationally more expensive than those using

*Often σ_h is referred to as σ_y.

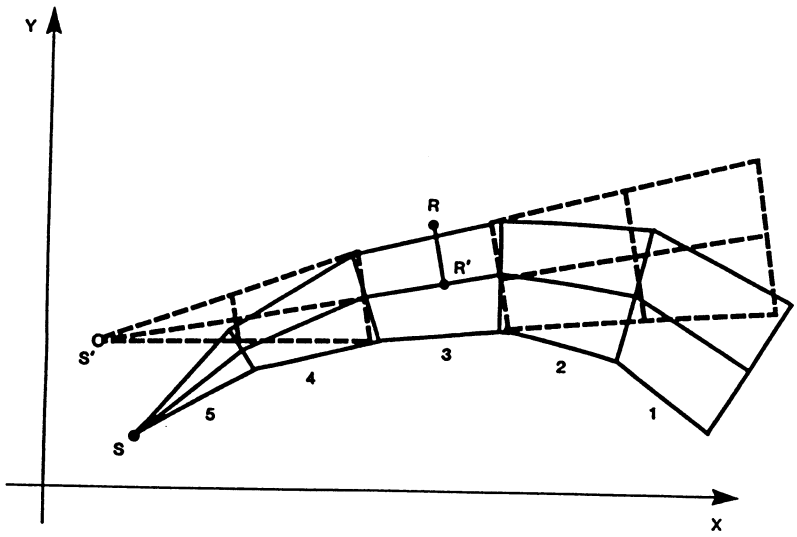

Fig. 1. Computation of the concentration at the receptor R generated by the segmented plume (solid lines). The computation is performed by evaluating the contribution of the virtual plume (dotted lines) from the virtual source S' passing through the closest segment (number 3) to the receptor R.

the segmented approach. In fact, a sufficient number of puffs must be generated so that the continuous plume is represented with enough accuracy by the superimposition of several puffs' contributions. For receptors close to the source this may require the generation of a new puff every few seconds. The puff computational cost is justified only when the extra capabilities of the puff approach are required; that is (1) during low-wind conditions which segments cannot handle, and (2) when different sections of the same plume affect a receptor, a situation which is treated in a straightforward way by the puff model, but which requires complex geometrical investigations with the segmented approach. In other cases, for example in common transport conditions, the segmented model is computationally faster and equally accurate.

This paper presents a mixed segment–puff numerical technique aiming at the joint utilization of both approaches, in a way which is both consistent with the physics of the atmospheric dispersion phenomena and computationally efficient. This method is implemented into a new version (Release 3) of the AVACTA II air quality diffusion package. This numerical method is described in section 2, while section 3 presents some details of puff/segment concentration computation. Finally, section 4 summarizes the general features of the AVACTA II computer package. Two appendices are included at the end of the paper. Appendix A describes a methodology for evaluating the σ_h and σ_z growth during calm or low-wind conditions, while Appendix B presents a preliminary comparison between AVACTA II outputs and (1) concentrations computed using the standard Gaussian steady-state equation; (2) SF_6 tracer diffusion experiments.

2. THE SEGMENT/PUFF APPROACH

This new approach is a dynamic one, in which each plume is described by a series of 'elements' (segments or puffs) whose characteristics are updated at each 'dispersion' time interval Δt (for example, 5–10 min). Meteorological three-dimensional fields (wind and turbulence status) and emission parameters are allowed to change at each 'meteorological' time step Δt_m (typically, 30–60 min). The dynamics of each element consist of (1) generation at the source; (2) plume rise; (3) transport by advective wind; (4) diffusion by atmospheric turbulence; (5) ground deposition, dry and wet; and (6) chemical transformation, creating secondary pollutant from a fraction of the primary pollutant. The type of element (segment or puff) does not affect its dynamics, but only the computation of the concentration field, which is discussed in section 3.

Each element is characterized by the following time-varying parameters (see the example in Fig. 2) evaluated at its final central point B:

$\mathbf{e} = (x_e, y_e, z_e)$	coordinates (m) of the point B;
h_e	elevation (m) of B above the ground (in flat terrain $h_e = z_e$);
M_1, M_2	masses of primary and secondary pollutant (kg);
$\sigma_h, \sigma_{z1}, \sigma_{z2}$	standard deviations (m) of the Gaussian concentration distribution: horizontal, vertical below B, and vertical above B, respectively.

The characteristics of each element's initial central point A at time t are equal to those, at the same time t,

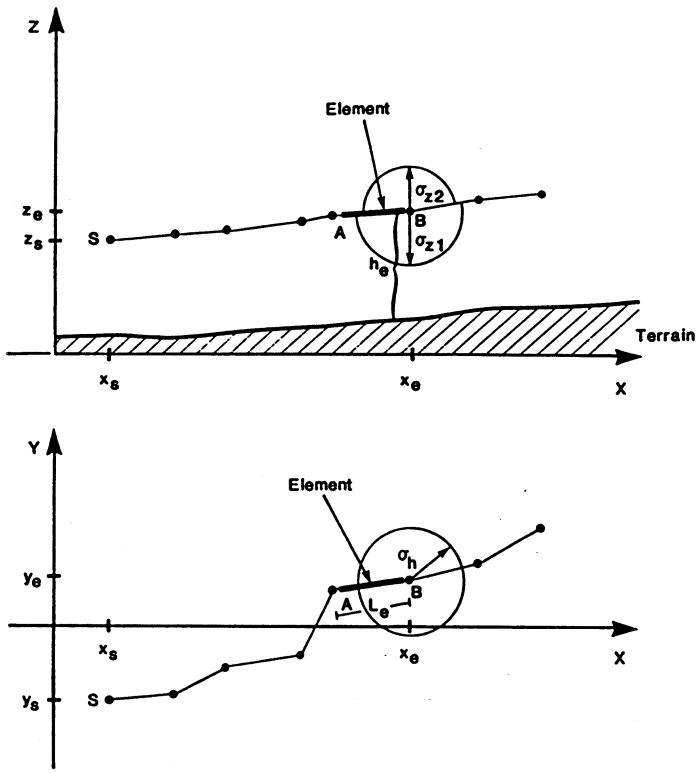

Fig. 2. Chain of elements from the source S at time t. The time-varying parameters of a selected element in the chain are illustrated.

of the final central point of the element successively emitted from the same source.

2.1. *Generation of plume elements*

At each time interval Δt, a new element is added to the element 'chain' from each source. The parameters defining each new element have the following initial values: the central final point is set at the source's exit point plus the vertical plume rise Δh; $M_1 = Q_1 \Delta t$, $M_2 = Q_2 \Delta t$, where Q_1 and Q_2 are the current emission rates of primary and secondary pollutants (generally $Q_2 = 0$); and σ_h, σ_{z1} and σ_{z2} represent the initial σs of the plume (for example, 0.369 multiplied by the source exit diameter may be chosen for σ_h, and $\Delta h/3.16$ for σ_{z1} and σ_{z2}).

2.2. *Transport*

At each time interval Δt, the central final point of each existing element is advected according to the current wind vector $\mathbf{u} = (u_x, u_y, u_z)$ averaged over the volume covered by the element size (i.e. $\pm 2\sigma$), as follows

$$\mathbf{e}^{(\text{new})} = \mathbf{e}^{(\text{old})} + \mathbf{u}\,\Delta t. \tag{3}$$

However, if the horizontal transport term

$$u_h = (u_x^2 + u_y^2)^{1/2} \tag{4}$$

is less than a critical value u_{min} (for example, $u_{min} = 1\ \text{m s}^{-1}$), u_x and u_y are forced to zero since it is assumed that such small terms represent more local intermittent effects than actual transport. In this case, however, a large horizontal diffusion may be produced by the large wind direction fluctuations typically encountered during these low wind speed situations (see the next section).

Moreover, the computerized version of this algorithm includes special user-supplied controls on z_e for avoiding unreasonably large variations of h_e, either in complex terrain simulations or during situations characterized by large u_z values. In fact, the program's user can optionally keep the relative variation of h_e, at each computational time step, within fixed limits.

2.3. *Diffusion*

During each Δt the element's σs are increased based on the virtual distance/age concept (Ludwig *et al.*, 1977; Zannetti, 1981) which operates for either σ_h, σ_{z1} or σ_{z2}, according to the following scheme, whose semi-empirical justification is presented in Appendix A,

1. select the current σ function $\sigma = \sigma(d)$ for the element (d is the downwind distance) according to the current local meteorology at the element's location; that is, the average atmospheric turbulent status* in the volume covered by the element size;

*The atmospheric turbulence status is often simply represented by a 'stability' class, a discrete number.

2. evaluate the virtual distance d_v such as

$$\sigma^{(old)} = \sigma(d_v) \quad (5)$$

where $\sigma^{(old)}$ is the current σ value for the element. The computation in Equation (5) is straightforward for some σ formulas (for example, power laws), but requires iterative procedures for others;

3. if $u_h < u_{min}$ force $u_h = u_{min}$;
4. increment σ by

$$\sigma^{(new)} = \sigma(d_v + u_h \Delta t). \quad (6)$$

The above dynamics of the σs depend upon the choice of the σ function and the current atmospheric turbulence status at the element's location. A separate turbulence status can be considered for the computation of horizontal (σ_h) and vertical (σ_{z1}, σ_{z2}) increments, if a proper meteorological input is available. For example, the temperature vertical gradient might provide an evaluation of the 'vertical' turbulence status, while the horizontal wind direction fluctuation intensity provides a good estimate of the 'horizontal' turbulence status. (It must be pointed out that, without the measurement of the horizontal wind direction fluctuation, the estimate of the 'horizontal' turbulence status may be quite wrong and provide horizontal diffusion rates that are much lower than the actual ones.) Different values of the vertical turbulence status above and below the element center generate different dynamics for σ_{z1} and σ_{z2}.

In the software implementation of the above diffusion algorithms, several options are provided to the user for computing the dynamics of the σs (e.g., the growth of σ_{z1} and σ_{z2} may be restricted after the plume becomes well mixed through the boundary layer).

2.4. *Dry and wet deposition*

Both dry and wet deposition for the primary and secondary pollutants are simulated by first-order reaction schemes and are computed during each Δt (s) by an exponential reduction of the pollutant mass (kg)

$$M_i^{(new)} = M_i^{(old)} \exp[-P_{i,j}\Delta t/360{,}000] \quad (7)$$

where i indicates the primary ($i = 1$) or the secondary ($i = 2$) pollutant, j indicates dry ($j = 1$) or wet ($j = 2$) deposition, and $P_{i,j}$ is the corresponding percentage of reduction per hour (% h^{-1}). All mass differences $M_i^{(old)} - M_i^{(new)}$ are deposited and accumulated on the ground.

If the two $P_{i,1}$ are not directly specified as input values, they can be obtained from the deposition velocity values as

$$P_{i,1} = 360{,}000\, V_i/\Delta z_e \quad (8)$$

where V_i are the current deposition velocities (m s^{-1}) at element's location, and $\Delta z_e = (2\sigma_{z1} + 2\sigma_{z2})$ is the vertical thickness (m) of the element. Equation (8) applies only when the plume has reached the ground (that is, $2\sigma_{z1} \geq h_e$), otherwise $P_{i,1} = 0$.

If the two $P_{i,2}$ are not directly specified as input values, they can be obtained (Draxler and Heffter, 1981) from precipitation data as

$$P_{i,2} = S_i P_r/(10 T_p) \quad (9)$$

where S_i are the pollutant scavenging ratios, P_r is the current average precipitation rate at element's location (mm h^{-1}), and T_p is the thickness (m) of the precipitation layer.

In the software implementation of the above deposition algorithm the parameters $P_{i,j}$ and the precipitation rate P_r are allowed to vary with time and space.

2.5. *Chemical transformation*

During each Δt (s), a first-order chemical reaction scheme is adopted, in which the chemical transformation term reduces the mass M_1 of primary pollutant and increases the mass M_2 of secondary pollutant in each element according to

$$M_1^{(new)} = M_1^{(old)} \exp(-k\Delta t/360{,}000) \quad (10a)$$

$$M_2^{(new)} = M_2^{(old)} + (w_2/w_1) M_1^{(old)} \times [1 - \exp(-k\Delta t/360{,}000)] \quad (10b)$$

where k is the current chemical transformation factor at the element location expressed as a percentage of reduction per hour (% h^{-1}), and w_i are the pollutant molecular weights ($i = 1, 2$).

3. CONCENTRATION COMPUTATION

As discussed in the previous section, plume element dynamics can be computed independently from the type of element (segment or puff). The element type however is a key factor in computing the plume concentration field during each Δt. The criterion for identifying the type of element is the ratio between its length L_e (the horizontal distance between A and B in Fig. 2) and σ_h. For a segment

$$L_e/\sigma_h > 2 \quad (11a)$$

and, for a puff,

$$L_e/\sigma_h \leq 2 \quad (11b)$$

where the center of the puff is located in the middle between A and B. Since σ_h continues to grow with time, all segments will eventually become puffs.

The above algorithm assures that, when segments are transformed into puffs, the distance between two consecutive puffs will not be greater than $2\sigma_h$, which is the condition required (Ludwig *et al.*, 1977) for a series of puffs to provide an almost perfect representation of a continuous plume. In calm or low wind speed conditions, $L_e = 0$ and puffs are generated directly from the source.

The above scheme allows a realistic and computationally efficient representation of calm, transport and transitional cases. For example, puffs can accumulate for a few hours in the region near the source during calm conditions, and then be subsequently

advected downwind when the stagnation breaks up. The concentration at each receptor point R due to a certain source S must account for the contribution of all elements generated from S; specifically, the sum of the contributions of all existing puffs plus the contribution of the closest segment. This allows a proper dynamic representation of both calm and transport conditions, including the previously mentioned situation in which, due to a 180° change in wind direction, two sections of the same plume may affect the same receptor. In this latter case, in fact, we can generally assume that the elements of the oldest section of the plume have already become puffs, thus allowing both sections of the plume to contribute to the concentration computation at that receptor.

3.1. *Puff contribution*

The concentration contribution of a single puff at a receptor R during each Δt is basically computed by Equation (2), which allows the computation of the primary pollutant concentration χ_1 (or the secondary one χ_2) from the current values of the puff's variables M_1 (or M_2), σ_h, σ_{z1} (or σ_{z2} if R is above the center of the puff), evaluated by interpolation at the center of the puff, that is the point between its initial and final central points. (It must be remembered that only if the puff has been generated during calm or low-wind conditions, that is, with $u_h = 0$, will its final and initial points coincide.) In the example of Fig. 2, the selected element is indeed a puff since $L_e < 2\sigma_h$, and its central point $\mathbf{p} = (x_p, y_p, z_p)$ is located in the middle between A and B.

3.2. *Segment contribution*

Because of the condition defined in Equation (11a) each segment has sufficient length L_e to assure that horizontal 'stream-wise' diffusion (that is, diffusion along the length of the segment) can be neglected in comparison with the transport term. This is one of the basic assumptions for Equation (1), which is used as the numerical algorithm for computing the concentration field due to a plume segment. This computation requires the identification of the segment closest to the receptor R and the utilization of the segment's variables for computing, using basically Equation (1), the concentration field generated by the equivalent plume passing through the segment, as illustrated in Fig. 1. The parameters in Equation (1) are evaluated in the following way:

1. segment's variables (M_1, M_2, σ_h, σ_{z1}, σ_{z2}) are interpolated at the point R' (see Fig. 1), the closest point to R along the segment centerline;
2. Q is evaluated as a virtual current emission rate; that is, $Q = M_1/\Delta t$ (or $M_2/\Delta t$);
3. u is evaluated as a virtual current wind speed; that is, $u = L_e/\Delta t$ (however, u is forced to be $\geq u_{min}$ to avoid unrealistic 'convergence' effects);
4. σ_{z2} is used instead of σ_{z1} if the receptor R is above the point R'.

Naturally, only the closest segment is used since its contribution surrogates that of the entire segmented portion of the plume.

3.3. *The treatment of the segment–puff transition*

The concentration computation described in the previous section allows the incorporation of all the

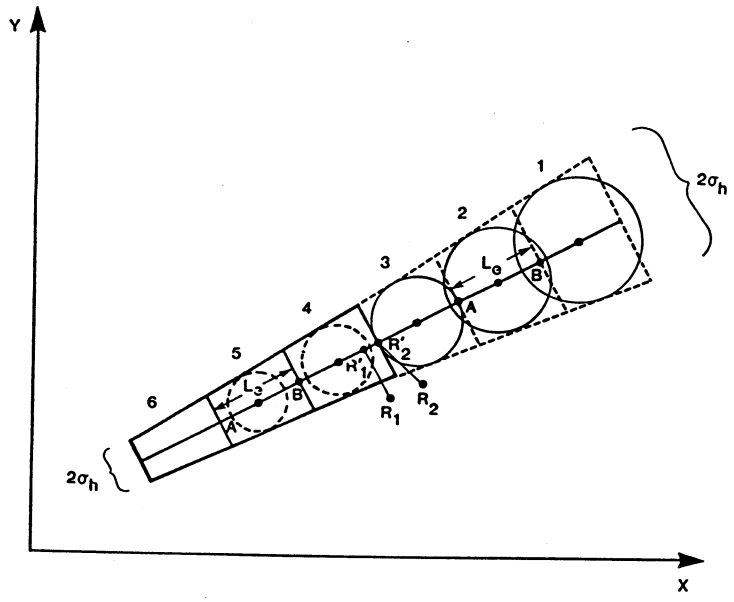

Fig. 3. Chain of elements and special treatment of the transition segment–puff. The contribution of the puffs 2 and 3 is eliminated for computing the concentration in R_1. The two segments 4 and 5 are transformed into puffs for computing the concentration in R_2.

advantages of both the puff and the segmented approach. Numerical problems, however, arise when the receptor is close to the point in the plume at which segments grow into puffs. In this case (see Fig. 3), care must be taken to avoid an inappropriate overevaluation of the concentration, since the concentration produced by the closest segment surrogates the effect of both the preceeding segments (elements 4, 5 and 6) and the following puffs (elements 1, 2 and 3).

The correct numerical treatment of this case requires the following operations for computing the concentration field:

1. if, during Δt, a segment becomes a puff (or vice versa), the element is treated as a puff;
2. in the case of receptor R_1 in Fig. 3, the contribution of the two puffs preceeding or following the closest segment is eliminated (unless the puffs have $L_e \leqslant \sigma_h/5$, which practically means that they have been generated in calm conditions; in this latter case their contribution is not eliminated);
3. in the case of receptor R_2 in Fig. 3, the closest segment and the segment eventually adjacent to it are treated as puffs.

Numerical tests have been performed which have shown that the above algorithms produce a 'smooth' concentration field, in which segment–puff transitions do not reduce the accuracy of the simulation.

3.4. *Splitting of elements*

The breaking of a plume into elements allows the evaluation of their dynamics as a function of the local time-varying meteorological conditions. In particular, during each Δt, the final central point of each element moves from an old to a new position. The horizontal

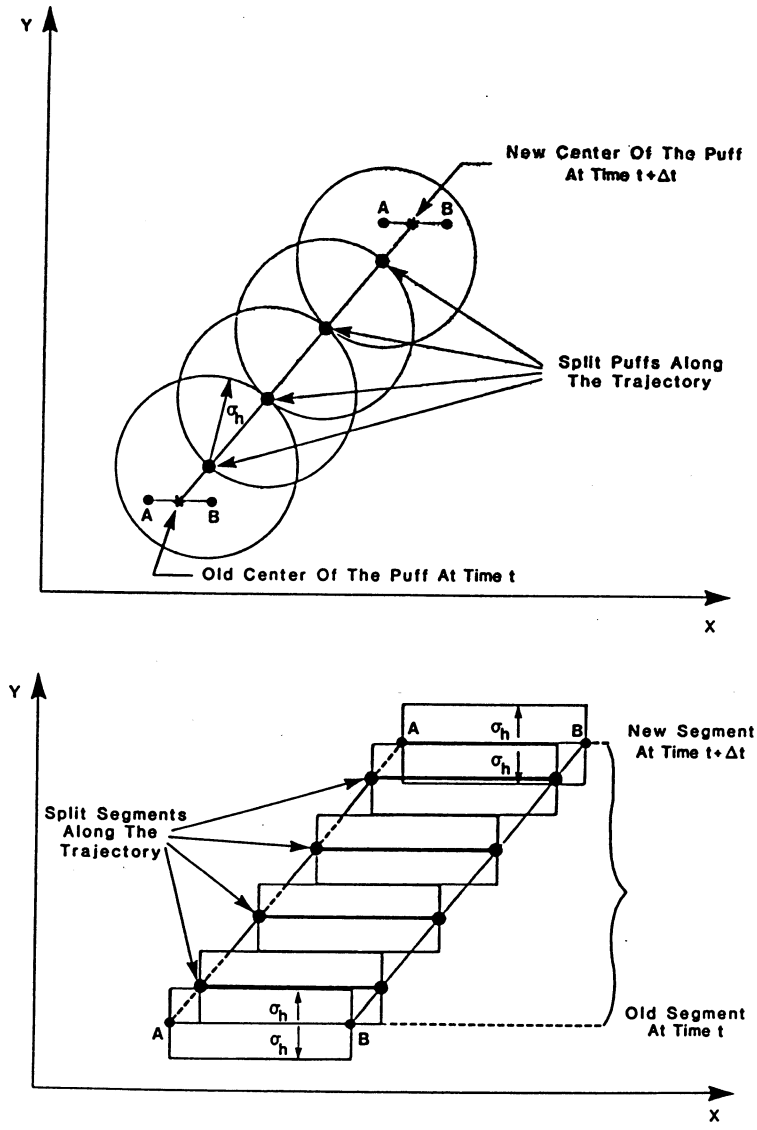

Fig. 4. Splitting process for a puff (above) and a segment (below). *A* and *B* again represent the initial and final central point of the element.

component of this advective displacement is

$$\Delta \mathbf{d}_h = \mathbf{u}_h \Delta t \quad (12)$$

where $\mathbf{u}_h = (u_x, u_y)$ is the current local horizontal wind vector.

Large $|\Delta \mathbf{d}_h|$, due to an increase in wind speed or associated to a change in wind direction, may affect the elements' ability to represent the continuous plume by reducing resolution. The splitting technique, which was originally proposed for puff modeling simulations (Zannetti, 1981), is here incorporated for both puffs and segments and is illustrated in Fig. 4. This splitting generates, when required, a sufficient number of fictitious elements along the element's trajectory during Δt to maintain sufficient resolution. The splitting of an element's trajectory is performed for computing its concentration contribution at receptor R when (1) the receptor R is affected by that element, and (2) for puffs, when $|\Delta \mathbf{d}_h| > \sigma_h$ and, for segments, when $|\Delta \mathbf{d}_t| > \sigma_h$, where $\Delta \mathbf{d}_t$ is the component of $\Delta \mathbf{d}_h$ that is transverse to the segment's centerline.

In this splitting computation the masses M_1 and M_2 of the element are equally distributed among the split elements along the trajectory from the old position to the new one.

4. THE AVACTA II COMPUTER PACKAGE

The methodology described in the previous sections has been incorporated into a computer program by expanding and re-structuring the Gaussian segmented package AVACTA II (Chan and Tombach, 1978; Zannetti *et al.*, 1981). The new version (Release 3) of the AVACTA II code incorporates the presented algorithms and, moreover, gives the user large flexibility in (1) defining the computational domain, the three-dimensional meteorological and emission input, and the receptor locations; and (2) selecting plume rise formulae, the σ functions and other options. Without explicit user's specifications, standard default values and assumptions are used.

The program is mainly designed for simulating air quality impact from point sources. However, due to its capability of treating sources with an initial $\sigma_h, \sigma_{z1}, \sigma_{z2}$, AVACTA II can also be correctly used for area and volume sources.

A full description of the AVACTA II software can be found in the user's manual (Zannetti *et al.*, 1985b). The major user's options currently implemented in AVACTA II allow the following:

a. selection of one of the following plume rise formulae:
   1. Briggs (Stern, 1976)
   2. CONCAWE (Stern, 1976)
   3. Lucas-Moore (Moore, 1974)
   4. Δh subroutine provided by the user;
b. selection of one of the following σ_z functions:
   1. Pasquill–Gifford–Turner (in the functional form specified by Green *et al.*, 1980)
   2. Brookhaven (Stern, 1976)
   3. Briggs, open country or urban (Gifford, 1976)
   4. LO-LOCAT (MacCready *et al.*, 1974)
   5. σ_z interpolated from user's values specified at fixed downwind distances (100 m, 1 km, 10 km, 100 km) and for each stability
   6. σ_z subroutine provided by the user;
c. selection of a σ_h function, independently from the σ_z choice (same selection as for σ_h, with the additional σ_h function from Irwin, 1979);
d. selection of different reflection assumptions; for example, partial reflection, total reflection with the Yamartino (1977) method, etc.;
e. direct specification of the meteorological input or the optional utilization of a special module (WEST module; Fabrick *et al.*, 1977) for evaluating, from meteorological measurements, a three-dimensional non-divergent wind field in either flat or complex terrain;
f. optional automatic generation of receptors on a user's specified grid (in rectangular or polar coordinates);
g. control of the element's vertical motion for avoiding unrealistic displacements, especially in complex terrain conditions.

The output of AVACTA II provides a full set of statistics of the concentration time series simulated at the receptor points (for both the primary and the secondary pollutants), and the dry deposition and wet deposition fields on a user selected grid. These statistics comprise hourly concentration values, 3-h and 24-h running concentration averages, and hourly, 3-h and 24-h total highest and highest–second-highest concentrations.

Acknowledgements—The author is grateful to the Center for Thermal and Nuclear Research (CRTN) of the National Electric Power Industry (ENEL) in Milan, Italy for their partial support of this study. Dr Gabriele Carboni, of CRTN-ENEL, provided important help and support, especially for the implementation of the model computer code and its user's manual. Appreciation is extended to Ms Roberta Lewis and Dr Ivar Tombach, of AeroVironment Inc., for their editorial review and useful discussions, and to Ms Barbara McMurray for typing the manuscript. The contribution of Cathedral Bluffs Shale Oil Company (Grand Junction, CO) to the early development of AVACTA II is gratefully acknowledged.

REFERENCES

Benkley C. W. and Bass A. (1980) Development of mesoscale air quality simulation models, Vol. 3. User's Guide to MESOPUFF (Mesoscale Puff) model. EPA 600/7-80-058, U.S. Environment Protection Agency, Research Triangle Park, NC.

Chan M. W., Head S. J. and Machiraju S. (1979) Development and validation of an air pollution model for complex terrain application. Paper presented at NATO/CCMS Air Pollution Pilot Study, Rome, Italy. AeroVironment Technical Paper No. 9559.

Chan M. W. and Tombach I. H. (1978) AVACTA—air pollution model for complex terrain applications. AeroVironment Inc., Pasadena, CA. Rep. AV-M-8213.

Draxler R. R. and Heffter J. L. (1981) Workbook for estimating the climatology of regional-continental scale atmospheric dispersion and deposition over the United States. NOAA Technical Memorandum ERL ARL-96.
Fabrick A., Sklarew R. and Wilson J. (1977) Point source model evaluation and development study. Science Applications Inc. Report for the California Air Resources, Board and California Energy Resources Conservation and Development Commission, under Contract A5-058-87.
Gifford F. A. (1976) Turbulent diffusion-typing schemes: a review. *Nuclear Safety* **17**, 68–86.
Green A. E. S., Singhal R. P. and Venkateswar R. (1980) Analytic extensions of the Gaussian plume model. *J. APCA* **30**, 773–000.
Hales J. M., Powell D. C. and Fox T. D. (1977) STRAM—an air pollution model incorporating non-linear chemistry, variable trajectories, and plume segment diffusion. EPA 450/3-77-012. Environmental Protection Agency, Research Triangle Park, NC.
Irwin J. S. (1979) Estimating plume dispersion—a recommended generalized scheme. *Fourth Symposium on Turbulence, Diffusion and Air Pollution.* AMS, Reno, NV, January.
Lamb R. G. (1969) An air pollution model of Los Angeles. M.S. thesis, University of California, Los Angeles, [see Lamb R. G. and Neiburger M. (1971) An interim version of a generalized urban diffusion model. *Atmospheric Environment* **5**, 239–264].
Lewellen W. S. and Teske M. (1976) Second-order closure modeling of diffusion in the atmospheric boundary layer. *Boundary-Layer Met.* **10**, 69–90.
Liu M.-K. and Moore G. E. (1984) Diagnostic validation of plume models at a Plains site. EPRI Final Report, EA-3077, January.
Ludwig F. L., Gasiorek L. S. and Ruff R. E. (1977) Simplification of a Gaussian puff model for real-time minicomputer use. *Atmospheric Environment* **11**, 431–436.
MacCready P. B., Baboolal L. B. and Lissaman P. B. S. (1974) Diffusion and turbulence aloft over complex terrain. Preprint volume, *AMS Symposium on Atmospheric Diffusion and Air Pollution*, Santa Barbara, CA.
Martin D. O. (1971) An urban diffusion model for estimating long-term average values of air quality. *J. APCA* **21**, 16–23.
Moore D. J. (1974) A comparison of the trajectories of rising buoyant plumes with theoretical-empirical models. *Atmospheric Environment* **8**, 441–457.
Roberts J. J., Croke E. S. and Kennedy A. S. (1970) An urban atmospheric dispersion model. *Symposium on Multiple-Source Urban Diffusion Models.* Air Pollut. Control Office Publ. No. AP-86, pp. 6.1–6.72 (available from the author).
Sheih C. M. (1978) A puff pollutant dispersion model with wind shear and dynamic plume rise. *Atmospheric Environment* **12**, 1933–1938.
Stern A. C. (Ed.) (1976) *Air Pollution*, Vol. I. Academic Press, New York.
Turner D. B. (1970) Workbook for atmospheric diffusion estimates. EPA Rep. AP-26 (NTIS PB 191-482).
Yamartino R. J. (1977) A new method of computing pollutant concentration in the presence of limited vertical mixing. *J. APCA* **25**, 467–468.
Zannetti P. (1981) An improved puff algorithm for plume dispersion simulation. *J. appl. Met.* **20**, 1203–1211.
Zannetti P. (1984) New Monte Carlo scheme for simulating Lagrangian particle diffusion with wind shear effects. *Appl. Math. Modeling* **8**, 188–192.
Zannetti P., Carboni G. and Lewis R. (1985a) AVACTA II: User's Guide—Release 3. AeroVironment Inc. Technical Report 85/520.
Zannetti, P., Carboni G. and Ceriani A. (1985b) AVACTA II model simulations of worst-case air pollution scenarios in northern Italy. Paper presented at the NATO-CCMS *Fifteenth International Technical Meeting (ITM) on Air Pollution Modeling and Its Application*, St. Louis, MO.
Zannetti P., Perun V. S. and Chan M. W. (1981) AVACTA II: User's Guide—Release 1. AeroVironment Inc., Pasadena, CA. Technical Report AV-FR-81/598.

APPENDIX A

Let us assume that the dynamics of σ (for either σ_h, σ_{z1}, or σ_{z2}) are represented by a power law of the downwind distance; that is

$$\sigma(d) = a d^b \tag{A.1}$$

where the coefficients a and b depend upon the atmospheric turbulence status. Equation (A.1) is valid only during transport conditions (that is, $u_h \geq u_{min}$), and the current value $\sigma^{(old)}$ of σ for a given element at time t is a function of each different turbulence status that was encountered by the element along its trajectory.

If a and b represent the current values (at time t) of the coefficients at the element's location, $\sigma^{(old)}$ can be expressed by

$$\sigma^{(old)} = a d_v^b \tag{A.2}$$

where d_v is the 'virtual' downwind distance. More precisely, d_v is the distance that the element would have travelled to have the same $\sigma^{(old)}$ at time t if the atmospheric turbulence status had been stationary and homogeneous (that is, constant a and b) along the entire trajectory.

Equation (A.2) gives

$$d_v = (\sigma^{(old)}/a)^{1/b} \tag{A.3}$$

which allows the derivation of the new value of σ at time $t + \Delta t$ by

$$\sigma^{(new)} = a(d_v + u_h \Delta t)^b. \tag{A.4}$$

For calm conditions ($u_h \leq u_{min}$), the above formulation is not correct. In this situation, however, it can be correctly assumed that the dynamics of σ are represented by a power law of time, that is

$$\sigma(t) = a' t^{b'} \tag{A.5}$$

where the new coefficients a', b' depend again upon the atmospheric turbulence status. Similar to transport case, if a' and b' are the current values (at time t) of the coefficients, the current value $\sigma^{(old)}$ of σ can be expressed by

$$\sigma^{(old)} = a' t_v^{b'} \tag{A.6}$$

where t_v is the 'virtual' age of the element. More exactly, t_v is the length of time that the element would have existed to have the same $\sigma^{(old)}$ at time t, if the atmospheric turbulence status had been stationary and homogeneous (that is, constant a' and b') during the element's entire life.

Equation (A.6) gives

$$t_v = (\sigma^{(old)}/a')^{1/b'} \tag{A.7}$$

allowing the evaluation of the new σ at time $t + \Delta t$ by

$$\sigma^{(new)} = a'(t_v + \Delta t)^{b'}. \tag{A.8}$$

Available tracer experiments provide values of a, b for each turbulence status, thus allowing the application of Equations (A.3) and (A.4) for computing the dynamics of σs during each time step Δt characterized by transport conditions. Little or no experimental information is, however, available for calm conditions to evaluate a' and b' for each turbulence status.

To circumvent this lack of information, we analyze the special case of stationary and homogeneous turbulence conditions with $u_h = u_{min}$. In this case, both Equations (A.2) and (A.6) are valid, which gives

$$\sigma^{(old)} = a d_v^b = a' t_v^{b'}. \tag{A.9}$$

But, in this special case, d_v and t_v are the actual current downwind distance and age of the element, and therefore

$$d_v = u_{min} t_v \tag{A.10}$$

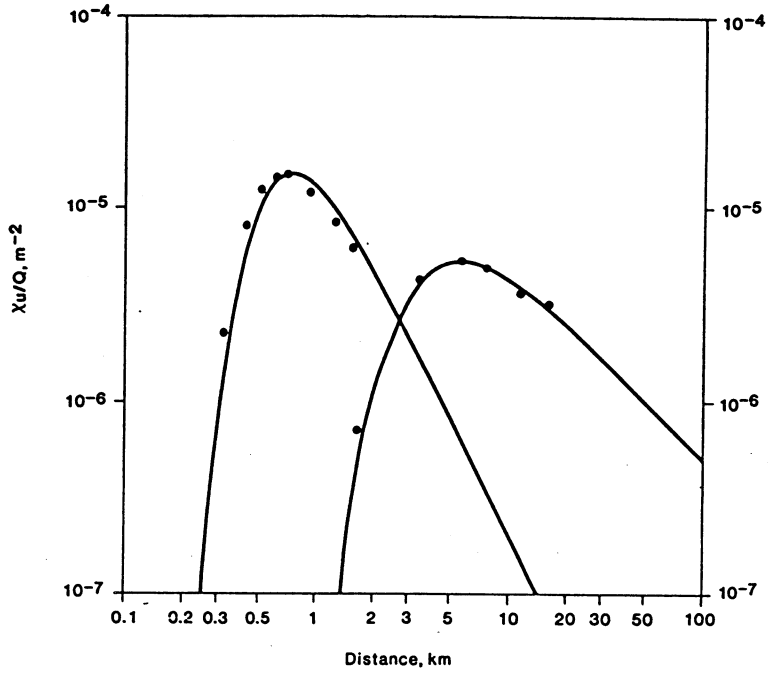

Fig. B.1. Comparison of AVACTA II outputs (dots) with standard Gaussian model results (curves from Turner, 1970). The two curves refer to the *B* stability (left) and *E* stability (right) class.

which, substituted in Equation (A.9), gives

$$a' = a u_{\min}^{b} \tag{A.11}$$

and

$$b' = b \tag{A.12}$$

which allow the evaluation of the coefficients a' and b' from the known coefficients a and b, for each corresponding atmospheric turbulent status.

Let us now focus on the element's dynamics at time t, independently from the possible non-stationary and non-homogeneous turbulence conditions that have characterized its dynamics before t. The element's σ dynamics are described by Equation (A.4) in transport conditions and by Equation (A.8) in low-wind conditions. By substituting Equations (A.7), (A.11), and (A.12) in the low-wind Equation (A.8) and remembering (A.3), we can rewrite (A.8) as

$$\sigma^{(\text{new})} = a(d_v + u_{\min}\Delta t)^{b} \tag{A.13}$$

which allows us to conclude that both transport and low-wind conditions can be simply treated by Equation (A.4) (which uses the known parameters a and b) by simply forcing $u_h = u_{\min}$ in low-wind conditions. The correct application of the method, however, requires the identification of the appropriate value for the transitional wind speed $u_{\min}$.

The four-step scheme presented in section 2.3 is a generalization of the above computations, using a general $\sigma(d)$ function, not necessarily expressed as a power law.

APPENDIX B

A full validation exercise is currently in progress, in which AVACTA II outputs will be compared with the data collected during several tracer diffusion experiments. This appendix presents some preliminary semi-quantitative evaluation of AVACTA II performance.

The model has been compared with standard Gaussian steady-state techniques and the AVACTA II capability of reproducing well, in stationary and homogeneous conditions, the output of standard Gaussian packages has been verified. An example of this comparison is illustrated in Fig. B.1.

Some preliminary AVACTA II simulations have been performed during two stagnant episodic conditions in Northern Italy (see Zannetti *et al.*, 1985b for a more detailed discussion). During the first episode (22 January 1982), a 3-h elevated SF_6 release was performed in the Turbigo area and ambient concentrations (30-min averages) were collected from 34 SF_6 ground-level monitors. AVACTA II showed some capability of evaluating (about half of the time) the maximum SF_6 concentration impact within a factor of two (but not necessarily at the same location where the maximum was measured). During the second episode (4–5 November 1981), AVACTA II was used to simulate the SO_2 ground-level impact from the emissions generated by the Turbigo power plant. The model performance was similar, but with a tendency to underpredict horizontal diffusion and overpredict concentration impacts.

While the above evaluation seems promising, these results confirm the difficulties in simulating stagnant, episodic conditions and the need of more modeling calibration effort.